Geophys. J. Int. (1999) **136,** 439–454

A spherical harmonic analysis of solar daily variations in the years 1964–1965: response estimates and source fields for global induction—I. Methods

Ulrich Schmucker
Geophysikalisches Institut der Universität Göttingen, Postfach 2341, D-37013 *Göttingen, Germany*

Accepted 1998 September 24. Received 1998 September 14; in original form 1998 March 4

SUMMARY

This work is based on a time harmonic and subsequent spherical harmonic analysis of daily variations, observed during 24 months at 94 magnetic observatories, 18 of them in the southern hemisphere. Observatories in polar or equatorial jet regions are not included. For global induction research this is a return to the classical potential method. It requires a dual spherical harmonic analysis of horizontal and vertical components, and thereby allows their separation into internal and external parts. The preceding time series analysis is a harmonic analysis of single Greenwich days, with a subsequent phase shift to zero time at local midnight. The selection of days is guided by the degree of magnetic activity, and the emphasis is on the analysis of quiet-time daily variations. To take full advantage of extended periods of quietness, a new measure is introduced, based on a fixed threshold for the sum of *ap* indices on the respective day and the adjoining half-days before and after.

The spherical harmonic analysis is carried out with time harmonics from all observatories except two, but weights are assigned to them to reduce their hemispherical imbalance. Time harmonics refer either to mean monthly daily variations or to those on single days. Noting that daily variations depend primarily on local time, the usual order of summations in spherical harmonic expansions is reversed. For each time harmonic, sums are formed over spherical terms of the same order m and ascending degree from $n = |m|$ onwards. The first partial sum is with $m = p$ for the local-time part of the pth time harmonic, the remaining sums with $m = p \pm 1$, $m = p \pm 2$, … for its part not moving with the speed of the Sun westwards. Up to the fourth harmonic, the spectrum of spherical harmonic coefficients is dominated by the second local-time term with $m = p$ and $n = p + 1$, except during solstices. For the fifth and sixth harmonics, this dominance is lost in all seasons.

The choice of spherical terms to be included has been guided by an eigenvalue decomposition of the normal equation matrix to ensure a numerically stable least-squares solution. No generalized inverse is used in order to allow a term-by-term determination of the expansion coefficients. In tests, the total number of terms has been varied between one and 36. Numerical instability sets in with a choice of more than 12 terms, notably in the expansion for the vertical field. With this number of terms, not more than one-half of the vertical field and about two-thirds of the horizontal field can be accounted for by spherical harmonics, in the global average. With a hypothetical network of comparable size, but with evenly spaced observing sites, all 36 terms could have been included.

Key words: electromagnetic induction, geomagnetic variation, spherical harmonics.

1 INTRODUCTION

Work on geomagnetic induction, extending investigations of the Earth's interior to include electric conductivity, began more than a hundred years ago with the analysis of daily variations. This is a fresh attempt to return to the classical potential method of those times and to demonstrate its undiminished viability under the favourable conditions that daily variations

provide. All modern works on the subject of global induction now use different methods, and in Part II an attempt will be made to compare and assess results for periods from one day to four hours. An interpretation with earth models of conductivity is not intended. It may be sufficient to state that this period range is relevant to mantle conductivities between 400 and 800 km depth.

This is also a return to the classical form of analysis, in which worldwide observed variation fields are approximated as functions of position by truncated series of spherical harmonics. In more recent developments, the use of spherical harmonics is either avoided altogether, as in the surface-integral method of Price & Wilkins (1963) where such fields are separated into external and internal parts, or they are replaced by spherical cap harmonics in order to separate surface fields within limited areas, as in the works of Haines & Torta (1994) and Torta & DeSantis (1996). The latter aim is also the purpose of Campbell's 'hemispheric mirror models' in various versions (Campbell 1990).

Extensive numerical experiments will be carried out with regard to the critical choice of days to be analysed, and with regard to the choice of spherical harmonics. Data from two years are used, and as many of the available observatories will be included as appear to be useful within the objectives of this study. The objectives are twofold: (1) to derive inductive response estimates for daily variations, but in a novel way with a least-squares univariate analysis of an assemblage of monthly means or single days; (2) to derive representative external field configurations for the four seasons. Their intended purpose is to provide electromagnetic model studies on a global scale with realistic source fields for induction. A first application to spherical models, which contain the irregular distribution of oceans and continents, forms the contents of a companion article by Kuvshinov, Avdeev & Pankratov (1999).

The external field studies are not directed towards gaining an understanding of the physical processes leading to the mainly ionospheric source currents. It is sufficient to recall that daily variations are basically connected to the Sun, even though a small portion arises from the Moon. The reduction to quiet-time daily variations of exclusively solar origin, denoted as *Sq variations*, will be part of the forthcoming analysis. Generally speaking, daily variations are quasi-periodic with the length of one solar day of 24 hours as the fundamental period. Their amplitudes undergo a distinct seasonal modulation. They are modified by magnetic activity and show, even during times of magnetic quietness, a small degree of day-to-day variability, of which only a minor part can be attributed to the changing phase of the Moon. The following introductory notes review the principles of the potential method and summarize its early results in conjunction with modern developments.

Ever since Schuster (1889) successfully separated daily variations into parts of external and internal origin it has been an established fact that these parts have a causal connection in accordance with the electromagnetic theory of induction: this is in terms of a skin effect upon slowly oscillating fields within conducting regions of the Earth. The external part from overhead currents acts herein as a primary source for secondary induced currents. The latter limit the downward penetration of the field into the Earth and cause, with their own magnetic field, the internal part.

It is essential to realize that the separation of the observed surface field into external and internal parts involves no other assumption except that this field can be regarded as a potential field; that is, no sources from the near-surface air-space contribute in any measurable way. This assumption is well founded in view of the extreme slowness of daily variations and the poor conductivity of the lower atmosphere. Hence, the term *potential method* is used when inductive response estimates are derived from internal to external relationships.

The lack of any assumptions with regard to the geometry of the Earth's conductivity distribution sets the potential method apart from all other methods, which avoid the problematic expansion of the surface field into spherical harmonics, at least for the particularly problematic vertical field component. Except for the magnetotelluric method, they proceed instead from the restrictive assumption of lateral uniformity in a certain space around the point of observation, in some cases also from a preset external source field geometry. The almost assumption-free magnetotelluric method has inherent problems of its own. They are connected to the mostly local character of the geoelectric field which tends to be present also at long periods. This view, however, may be biased by experiences on land.

The early success of the geomagnetic potential method seems to be due to two reasons. First, daily variations reoccur regularly day after day with considerable amplitude—they are the dominant feature on any magnetogram, in the absence of magnetic storms and at some distance from polar jet regions. Consequently, no elaborate time-series analysis is needed. It will be seen that the evaluation of a few days of magnetic quietness is sufficient to derive useful results. Second, daily variations have a smooth appearance in their global time–space structure, excluding again polar jet regions and now also the vicinity of the dip equator, where a localized electrojet enhancement of daily variations occurs. Hence, a small number of spherical terms, which can be derived from the limited number of available observation sites, is sufficient for an adequate global representation. Chapman (1919), in his most successful analysis of daily variations in the years 1902 and 1905, determined only one spherical term for each time harmonic. This was possible because he used local midnight as zero time reference and concentrated on daily variations around equinoxes, where symmetries with respect to the equator simplify the spatial structure.

The separation analysis of solar daily variations (S) was soon followed by a corresponding analysis of lunar daily variations (L). Furthermore, the aperiodic equatorial ring current field (Dst) during the recovery phase after magnetic storms was separated. In both cases, single-term source-field approximations are possible, and internal parts were found which, in their relation to the respective external parts, were in full support of what had been deduced already from S. For a review on these early results the reader is referred to Chapter XX of Chapman & Bartels' 'Geomagnetism' (1940).

Later, various attempts were made, notably by Rikitake (1950), to separate faster variations on a global scale, for example substorms or 'bay' disturbances. It could be expected that their short duration, and thus reduced depth of penetration, would provide more information about conductivity at shallow depth. However, their intimate connection to polar jets ruled out any adequate representation by a realistic number of spherical harmonics, and there is the additional complication

from the increasing influence of internal induction anomalies. It appears that no further attempts have been made to extend the potential method beyond its classical applications to S (Sq and S_D), L and Dst.

Even these applications, however, are not without their inherent problems. In the case of S they became evident when new separations were performed with many more observatories. Whereas Chapman (1919) used data from not more than 21 sites, the most recent investigations involved up to 130 observatories. As far as external to internal relationships were concerned, however, no substantial progress was made, although clearly most of these investigations had different priorities. Malin's (1973) analysis of the IGY/IGC data as well as Winch's (1981) analysis of the IQSY data were directed towards lunar daily variations, even though they included as a by-product solar daily variations, but only in the average over the entire time spans involved. A third major separation analysis, which will be cited repeatedly, is Parkinson's (1977) analysis of the IGY data. Even though it concentrates solely on Sq and was performed on a monthly basis, the results were so disappointing that Parkinson remarked in his conclusions 'that the conductivity distribution of the Earth's interior based on Sq must remain in some doubt'.

A more optimistic view has been expressed by Chapman & Bartels (1940; Section 22.1). Their main concern was the uncertain influence of oceans on the internal part of S. Consistent results from three different source fields (S, L, Dst), involving almost one decade in frequency, convinced them, however, that the distorting effect of oceans and perhaps other deep-seated irregularities cannot be so great as to invalidate the observed compatibility of the three sets of response estimates with laterally uniform earth models. This encouraging outlook has been the main source of inspiration to return once more to the potential method.

In this first article of two the emphasis will be on methodical aspects and data selection, while the second article (Schmucker 1999), henceforth referred to as Part II, presents results for the two stated objectives of this study.

2 THE IQSY DATA

As a follow-up of the International Geophysical Year (IGY) of 1957–1958 with maximum sunspot numbers, the years 1964–1965 of minimum solar activity have been declared as International Quiet Sun Years (IQSY) of worldwide cooperation. In a great effort, Dr Winch has been able to assemble geomagnetic data for these two years from 130 observatories and to arrange for their transfer into computer-readable form, after a thorough review. These data, comprising 6.8 million hourly means from observatory yearbooks, will be analysed. This repeats to some extent Winch's (1981) own analysis, but now the emphasis will be on solar rather than lunar daily variations and the focus is on induction.

The data set is not complete. In addition to numerous gaps, in some cases for several months in a row, nine observatories have only the 1964 data and fourteen only those of 1965. To the latter, 10 observatories could be added from Dr Fainberg's collection, augmenting in three cases existing 1964 data. Short gaps of not more than six hours were closed by interpolation and all data were reviewed once again.

Monthly plots displayed such a high degree of similarity among neighbouring sites that questionable values could be detected by visual inspection and comparison. About 1200 new corrections were made, whenever faulty entries were obvious. These were typically permutations of digits (743 instead of 473 in a sequence 476 474 743 470), wrong hundreds or, during sufficient quietness, also tens (798 instead of 698 in a sequence 712 706 798 705; 549 instead of 539 in a sequence 542 541 549 540). The quoted numbers are in units of nanotesla or tenths of a degree of arc. The new data collection has been re-submitted for further use to the World Data Center, with a full documentation of all executed changes.

As a rule, the geomagnetic elements' horizontal intensity (H), declination (D) and vertical intensity (Z) were tabulated. When converting H and D into the north component $X = H \cos D$ and the east component $Y = H \sin D$ in geographical coordinates, special attention was given to the possibility that the tabulated entries of D refer to western rather than eastern declination. A similar ambiguity in the sign of Z in the southern hemisphere has already been resolved by Dr Winch. It appears that all entries are, correctly, mean values centred halfway between full hours in Universal time.

Data from observatories close to polar or equatorial jets will not be used for reasons stated in Section 6. After various trial runs, 60° geomagnetic latitude was adopted as the upper limit for inclusion in high latitudes, and 6° dip latitude as the lower limit for inclusion near to the equator. This eliminates 36 high-latitude observatories and seven at low latitudes. Of the remaining 94 observatories, 18 are in the southern hemisphere and 35 are located on islands or close to coast lines in the sense that the nearest distance to the 2000 m depth contour is less than 300 km. Exceptions from this rule are observatories on the east coast of South America, which are classified as 'coastal', even though the deep Atlantic may be further away than 300 km. On the other hand, all Iberian and Italian observatories are counted as 'continental', independent of their distance to the 2000 m depth contour in the Mediterranean Sea. This includes Logrono in northern Spain, which is just 150 km away from the deep waters in the Bay of Biscay. Full information is listed together with the observatory acronyms and geographical coordinates in Table 1. Fig. 1 displays their positions on a global map.

3 THE DERIVATION OF SINGLE-DAY TIME HARMONICS

Time harmonic and spherical harmonic analyses will follow each other in this order; that is, the development into series of spherical harmonics is carried out with individual time harmonics of daily variations. The chosen sequence of operations does not matter in principle, although in practice different sets of spherical harmonics will be used for different time harmonics, which renders the sequence of operations irreversible.

It would not be advisable to analyse long unbroken series of hourly values, extending over several days, because daily variations vary in their appearance and their spatial configuration from day to day, mostly in dependence on magnetic activity. Therefore single days will be analysed. This influential decision should be seen in the context of Sq and S_D contributions to daily variations, where S_D denotes the difference between daily variations on disturbed and quiet days, in a monthly average. Only quiet-day Sq variations have the desired smoothness in dependence on latitude and longitude, whereas S_D increases steeply in amplitude towards the polar jets as

Table 1. Names and geographical coordinates of IQSY geomagnetic observatories.

Yakutsk	YAK	62.02 N	129.67 E	6	C	2
Nurmijarvi	NUR	60.52	24.65	6	C	1
Leningrad	LNN	59.95	30.70	6	C	1
Lovö	LOV	59.35	17.83	6	C	1
Sitka	SIT	57.07	224.67	6	I	2
Sverdlovsk	SVD	56.73	61.07	6	C	1
Tomsk	TMK	56.47	84.93	5	C	2
Rude Skov	RSV	55.85	12.45	6	C	1
Kazan	KZN	55.83	48.85	6	C	1
Moscow	MOS	55.48	37.32	6	C	1
Eskdalemuir	ESK	55.32	356.80	6	C	1
Minsk	MNK	54.10	26.52	6	C	1
Stonyhurst	STO	53.85	357.53	6	C	1
Wingst	WNG	53.75	9.07	6	C	1
Witteveen	WIT	52.82	6.67	6	C	1
Irkutsk	IRT	52.17	104.45	6	C	2
Swider	SWI	52.12	21.25	6	C	1
Niemegk	NGK	52.07	12.68	6	C	1
Valentia	VAL	51.93	349.75	6	I	1
Hartland	HAD	51.00	355.52	6	C	1
Kiev	KIV	50.72	30.30	6	C	1
Dourbes	DOU	50.10	4.60	6	C	1
Pruhonice	PRU	49.98	14.55	6	C	1
Lvov	LVV	49.90	23.75	6	C	1
Victoria	VIC	48.50	236.60	6	I	2
Wien-Kobenzl	WIK	48.37	16.32	6	C	1
Fürstenfeldbruck	FUR	48.17	11.28	6	C	1
Chambon-la-Forêt	CLF	48.02	2.27	4	C	1
Hurbanovo	HRB	47.87	18.18	6	C	1
Yuzhno-Sakhalinsk	YSS	46.95	142.72	6	I	1
Tihany	THY	46.90	17.90	6	C	1
Odessa	ODE	46.78	30.88	6	C	1
Surlari	SUA	44.68	26.25	6	C	1
Grocka	GCK	44.63	20.77	5	C	1
Roburent	ROB	44.30	7.88	5	C	1
Memambetsu	MMB	43.90	144.20	6	I	1
Agincourt	AGN	43.78	280.73	6	C	1
Vladivostok	VLA	43.68	132.00	6	I	1
Alma Ata	AAA	43.25	76.92	5	C	1
Panagyurishte	PAG	42.52	24.18	6	C	1
L'Aquila	AQU	42.38	13.32	6	C	1
Logrono	LGR	42.25	357.50	6	C	1
Tbilisi	TFS	42.08	44.70	6	C	1
Tashkent	TKT	41.33	69.62	6	C	1
Ebro	EBR	40.82	0.50	5	C	1
Coimbra	COI	40.22	351.58	6	I	1
Toledo	TOL	39.88	355.95	6	C	1
Frederichsburg	FRD	38.20	282.03	6	I	2
Ashkhabad	ASH	37.95	58.10	6	C	1
Almeria	ALM	36.85	357.53	6	C	1
San Fernando	SFS	36.47	353.80	6	I	1
Kakioka	KAK	36.23	140.18	6	I	1
Teheran	TEH	35.73	51.38	5	C	1
Simosato	SSO	33.57	135.93	6	I	1
Dallas	DAL	32.98	263.25	6	C	2
Tucson	TUC	32.25	249.17	6	C	2
Kanoya	KNY	31.42	130.88	6	I	1
Sabhawala	SAB	30.33	77.80	5	C	1
Quetta	QUE	30.19	66.95	5	C	1
Misallat	MLT	29.52	30.90	6	C	1
Teneriffa	TEN	28.48	343.72	6	I	1
Havanna	HVN	22.97	277.85	5	I	2
Cha-Pa	CPA	22.35	103.83	5	C	1
Honolulu	HON	21.32	202.00	6	I	2
Teoloyucan	TEO	19.75	260.82	5	C	2
San Juan	SJG	18.38	293.88	6	I	1
Alibag	ABG	18.63	72.87	6	I	1
Vieques	VQC	18.15	294.55	5	I	0 (XY) 1 (Z)
Hyderabad	HYB	17.42	78.55	5	C	1
M'Bour	MBO	14.40	343.02	6	I	2
Muntinlupa	MUT	14.37	121.02	6	I	2
Guam	GUA	13.58	144.87	6	I	2
Paramaribo	PAB	5.82	304.78	6	I	1
Fuquene	FUQ	5.47	286.27	6	C	2
Bangui	BNG	4.43	18.57	6	C	1
Moca	MFP	3.35	8.67	6	I	1
Tatuoca	TTB	-1.20	311.48	5	I	2
Nairobi	NAI	-1.28	36.82	5	C	2
Lwiro	LWI	-2.25	28.80	6	C	2
Tangerang	TNG	-6.17	106.63	6	I	0 (XYZ)
Luanda	LUA	-8.92	13.17	6	I	2
Port Moresby	PMG	-9.40	147.15	6	I	2
Apia	API	-13.80	188.22	6	I	2
Tananarive	TAN	-18.92	47.55	6	I	2
Tsumeb	TSU	-19.22	17.70	5	C	2
La Quiaca	LQA	-22.10	294.40	6	C	2 (XY) 0 (Z)
Pilar	PIL	-31.67	296.12	6	C	2
Gnangara	GNA	-31.78	115.95	6	I	2
Hermanus	HER	-34.42	19.20	6	I	2
Toolangi	TOO	-37.53	145.47	6	I	2
Amberley	AML	-43.15	172.72	4	I	2
Trelew	TRW	-43.25	294.68	5	I	2
Kerguelen	KGL	-49.35	70.22	6	I	2
Argentine Isl.	AIA	-65.25	295.73	6	I	2

Notes. Year code: 4 = 1964 only, 5 = 1965 only, 6 = 1964 & 1965.
Location code: C = continental, I = island or coastline.
Weight code: 0 = excluded, 1 = half weight, 2 = full weight.

their primary source regions. Because Sq and S_D are so different in their spatial structure, any analysis over sequences of days of varying activity would result in an unseparable mixture of two sources in unknown proportions. Substorm events of short duration, in comparison to daily variations, may still be present on the chosen days, but their effect is likely to disappear in the average. The removal of lunar daily variations will require special attention.

Three further decisions are necessary: with respect to coordinates, time reference and baseline. Since the Sun is the prime cause, geographical coordinates are a natural choice. However, the asymmetry of the Earth's permanent field with respect to the axis of rotation provides an argument for the use of geomagnetic coordinates because this field is responsible for the electromotive driving force of external source currents and also for the directional dependence of ionospheric conductivity. Tests have shown, however, that the choice of coordinates has only marginal influence on the fit by spherical harmonics, and geographical coordinates are used. The reason seems to be that the greatest complication of the global Sq system arises from the meandering course of the dip equator, which deviates from the geomagnetic equator nearly as much as from the geographical equator, as seen in Fig. 1.

Since the Earth rotates under external current loops which are fixed in space by the position of the Sun, daily variations should preferably be reckoned in local solar time $T = t + \lambda$ rather than in Universal time t, with λ as the geographical longitude of the point of observation. Hereafter, times are in angular measure with 2π corresponding to one full solar day of 24 hours. However, if at a given site the harmonic analysis were conducted in time intervals from local midnight to local midnight, then nearly no overlap would exist in real time for sites on either side of the datum line. Therefore it has been decided to perform the analysis on the Greenwich day with a subsequent shift of phases to local midnight.

In either case, a periodic continuation for at least 12 hr before and after the chosen Greenwich day is required, and special precautions will be taken in Section 5 to ensure that this entire time span of 48 hours is of reasonable magnetic quietness. As already pointed out by Price & Stone (1964), the adopted way of analysing single days implies for sites in the Far East or Far West that the time interval of analysis begins and ends near local noon. Therefore, non-cyclic changes, as defined below, could arise more from the day-to-day variability of daily variations than from the recovery phase of storms, as is usually presumed. This inconsistency has been accepted in order to perform the spherical harmonic analysis with data from exactly the same time interval everywhere.

The third decision concerns the reference level from which to measure daily variations on a given day. Since a time-

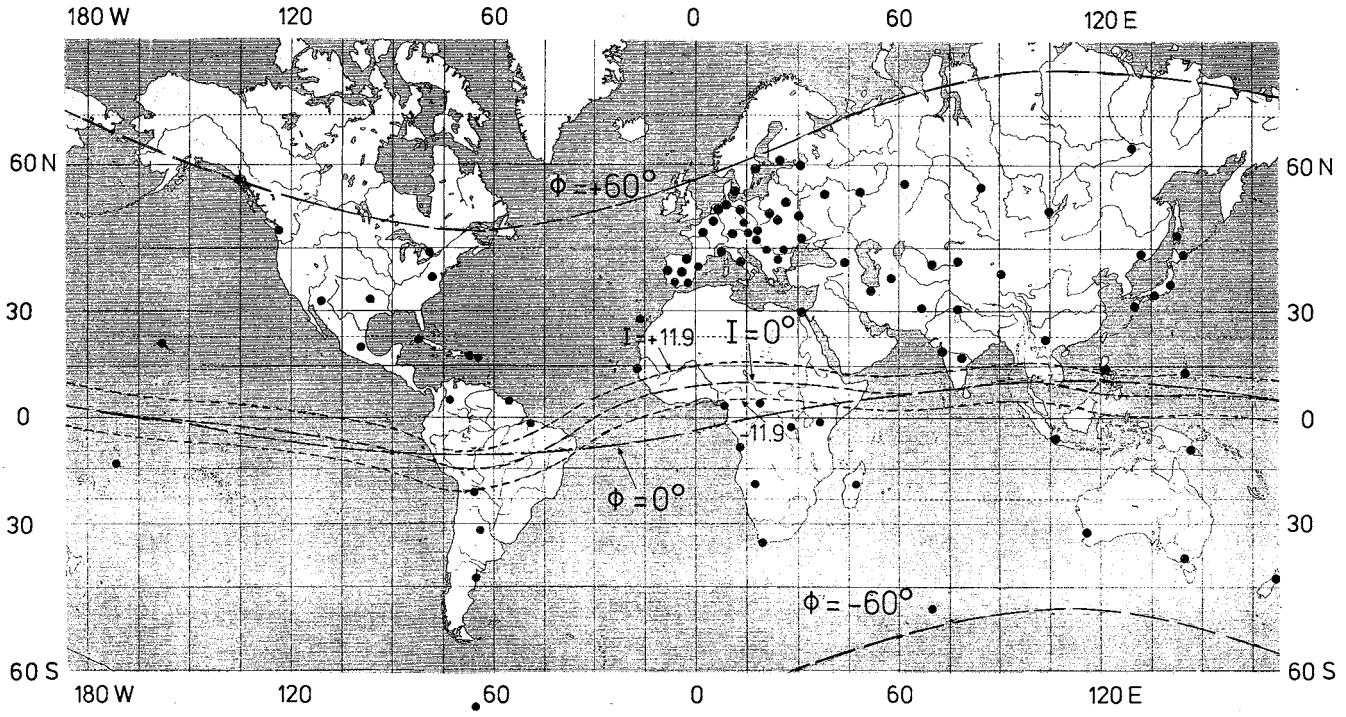

Figure 1. Positions of the selected 94 geomagnetic IQSY observatories of this study, in geographical coordinates. Towards the poles they are bound by lines of $\pm 60^\circ$ *geomagnetic* latitude Φ; towards the dip equator, by lines of $\pm 6^\circ$ *dip* latitude $\phi_{\rm dip}$ or $\pm 11.9^\circ$ main field inclination I, with $2tg\phi_{\rm dip} = tgI$. Within these limits, 76 observatories lie in the northern and 18 observatories in the southern hemisphere (*cf*. Table 1). Not shown are 36 polar and seven equatorial observatories with available, but unused, IQSY data.

constant field does not induce currents, the choice of this level is immaterial for induction studies, and any induction effects on a larger timescale than one day should have been removed by non-cyclic change corrections beforehand. The choice of reference level does matter, however, if external or internal fields or equivalent currents are to be constructed. Ideally, this 'baseline' should represent the undisturbed *true zero* level of *no* daily variations. The local midnight level may be close to that level, but only with respect to the external part. Ashour & Price (1965) have shown that during local midnight an internal field exists from induced currents crossing the midnight meridian, even when at this time the field from external currents is exactly zero, as presumed hereafter. Thus the following procedure has been chosen, which is similar to Parkinson's (1977) approach.

First, a smoothed midnight level is defined from the first three hours of the local *solar* day and subtracted from all hourly values of the chosen *Greenwich* day. Subsequently, the daily mean with respect to this local midnight level, that is the absolute term of the harmonic analysis, is split into external and internal parts, after an expansion into spherical harmonics. The resulting external part measures the distance of the daily mean (which has no internal part) from true zero, which is thus found. Similarly, the internal part reveals how far the midnight level deviates from true zero because of induction. Appendix A gives the details and also states the necessary assumptions involved.

Concerning the actual performance of the harmonic analysis note the following. Let, on the chosen Greenwich day, f_n be an hourly mean value for the interval which begins at the nth hour Universal time. With $n = 0, 1, 2, \ldots 24$, f_0 is the first value of this day and f_{24} the first value of the next. Their difference, $d = f_{24} - f_0$, defines the non-cyclic change of the chosen day. After replacing the first value by the mean $(f_0 + f_{24})/2$ (to follow the trapezoidal formula of numerical integration of the Fourier integral), the Fourier coefficients of the day are

$$A_p = \frac{2}{N}\sum_{n=0}^{N-1} f_n \cos(2\pi pn) \quad \text{and} \quad B_p = \frac{2}{N}\sum_{n=0}^{N-1} f_n \sin(2\pi pn), \tag{1}$$

when $p = 1, 2, \ldots (< N/2)$ denotes the pth harmonic of daily variations and $N = 24$. The first six harmonics will be derived.

Two corrections are needed: a trend correction for the non-cyclic change and one for the use of mean values instead of instantaneous values (Chapman & Bartels 1940; Sections 16.15 and 16.17):

$$B_p \to B_p + \frac{d}{N \tan \alpha}, \quad \text{and then} \quad A_p, B_p \to A_p \frac{\alpha}{\sin \alpha}, B_p \frac{\alpha}{\sin \alpha},$$

with $\alpha = \pi p/N$. The second correction has been applied only to retain the option for a time harmonic synthesis of instantaneous values. Phases of the harmonics are reckoned against one half-hour after midnight Universal time, but there is no need to correct them for exact reference to midnight.

The corrected harmonic coefficients A_p and B_p are then combined to form a complex Fourier amplitude, henceforth referred to as the pth time harmonic,

$$C_p = (A_p - iB_p)\, e^{ip\lambda}, \tag{2}$$

with a concurrent phase shift to local midnight as zero time reference. The harmonic synthesis yields in

$$f'_n = A_0 + \sum_p \mathscr{R}e\{C_p\, e^{2\pi i pn}\}, \quad \text{with } A_0 = \frac{1}{N}\sum_n f_n, \tag{3}$$

trend-corrected synthesized daily variations in the form of instantaneous values half-way between full hours in local time.

4 A SOURCE-ORIENTED SPHERICAL HARMONIC ANALYSIS OF DAILY VARIATIONS

The potential method requires two series expansions into spherical harmonics: the first for the magnetic potential U, to be conducted with the horizontal north and east components

$$X = +\frac{1}{R}\partial U/\partial\theta, \qquad Y = -\frac{1}{R\sin\theta}\partial U/\partial\lambda \tag{4}$$

of the magnetic surface field, and the second for the vertical magnetic field component $Z = +\partial U/\partial r$ at $r = R$. Geocentric coordinates (r, θ, λ) are used, and R is the Earth's radius: θ and λ are geographical co-latitude and longitude of a surface point of observation. The condition for deriving the magnetic field vector as (negative) gradient of a scalar potential has been stated in the Introduction.

Various options exist to formulate these series for the time harmonics of U and Z. If they have the stated purpose of expressing the external source field with its internal field by induction in an Earth that is nearly radially symmetric, then full advantage should be taken of the fact that daily variations in their major portion occur in local time. Consequently, for an observer on the rotating Earth they will consist predominantly of westward 'travelling waves', moving more or less with the speed of the Sun around the Earth from east to west: 15° in longitude per hour.

A minor part of daily variations should consist of 'standing waves'. Their origin is twofold: first because the Earth's permanent field deviates from axial symmetry with respect to the axis of rotation; second because the internal field will be affected by the presence of oceans and possibly other lateral inhomogeneities of conductivity within the Earth. In either case contributions to the surface field will arise, which are fixed to the rotating Earth. Note that the term 'wave' does not refer in this context to electromagnetic waves propagating with the speed of light, but to fields with time–distance factors $\exp\{i(\omega t + kx)\}$ which move in the negative x-direction of Cartesian coordinates when the wavenumber k is positive, and vice versa. In spherical coordinates, this factor corresponds to a time–longitude factor $\exp\{i(pt + m\lambda)\}$ for the pth time harmonic. Henceforth, the letters n and m denote degrees and orders of spherical harmonics. In the complex notation used here, m may be negative.

For the intended form of presentation by spherical harmonics, the usual order of summations first over degrees and then over orders is reversed, as outlined in Appendix B. Each time harmonic of U and Z is expressed by a series of partial sums with the above-mentioned time-longitude factors and thereby with fixed orders m of the spherical terms in them. Each partial sum contains K terms of ascending degree $n = |m|$, $|m| + 1, \ldots, |m| + K - 1$ for associated spherical functions $P_n^m(\cos\theta)$ to express dependence on co-latitude. By using the same K for all partial sums and with m in the range $[p - L, p + L]$, $L = 0, 1, \ldots$, the total number of terms is

$$M = K(1 + 2L). \tag{5}$$

The decision to give the partial sums all the same number of K terms has been guided by the fact that the spherical functions involved have then the same number of zeroes between poles and thereby similar shapes, for any fixed order. It should be added that whenever expansion coefficients are quoted in nanotesla, they refer to quasi-normalized spherical functions according to A. Schmidt. For these functions, spherical harmonics of positive and negative order are related as $P_n^{-m} = (-1)^m P_n^m$.

Explicitly, the series to be evaluated for the complex pth time harmonic of the potential is

$$U_p(\theta, \lambda)\,\mathrm{e}^{ipt} = R\left\{I_p(\theta) + \sum_{\ell=1}^{L} I_{p+\ell}(\theta)\,\mathrm{e}^{i\ell\lambda} + I_{p-\ell}(\theta)\,\mathrm{e}^{-i\ell\lambda}\right\}\mathrm{e}^{ipT}, \tag{6}$$

with R as the Earth's radius and $I_p, I_{p\pm1}, \ldots$ as partial sums to the orders $m = p$, $m = p \pm 1, \ldots$. For clarity, Universal time factors $\exp(ipt)$ have been included on both sides. On the right-hand side it has been combined with longitude factors $\exp(ip\lambda)$, split from $\exp(im\lambda)$ with $m = p \pm \ell$, to form a local-time factor $\exp(ipT)$ with $T = t + \lambda$. The latter can be omitted in the series for time harmonics of field components because these are reckoned in local time. Hence, the second series to be evaluated can be written simply as

$$Z_p(\theta, \lambda) = J_p(\theta) + J_{p+1}(\theta)\,\mathrm{e}^{i\lambda} + J_{p-1}\,\mathrm{e}^{-i\lambda} + J_{p+2}(\theta)\,\mathrm{e}^{i2\lambda} + J_{p-2}\,\mathrm{e}^{-i2\lambda} + \ldots. \tag{7}$$

By denoting the (complex) expansion coefficients for U by u_n^m and those for Z by z_n^m, the explicit expressions for the partial sums of the two series are

$$I_m(\theta) = \sum_{n=|m|}^{|m|+K-1} u_n^m P_n^m(\cos\theta) \quad \text{and} \quad J_m(\theta) = \sum_n z_n^m P_n^m(\cos\theta). \tag{8}$$

If needed, the association with a specific time harmonic will be added in parenthesis, for example $u_n^m(p)$.

The physical interpretation of partial sums is obvious. The first sums with $m = p$ represent the local-time part of daily variations, moving with the speed of the Sun westwards. They are therefore without longitude factors. The most stable and, except during solstices, largest term is the second *principal term* of degree $n = p + 1$, and this is the only term in Chapman's (1919) analysis during equinoxes. Hereinafter terms with $m = p$ are denoted as 'local-time terms' and those with $m \neq p$ as 'general terms'.

The following partial sums with $m = p \pm 1, p \pm 2, \ldots$ account for any remaining part of daily variations, not moving with the speed of the Sun westwards. Provided m is positive, they also represent westward-moving fields—those with $m > p$ travelling faster, and those with $0 < m < p$ travelling slower than the Sun. Partial sums of negative order are associated with parts of daily variations, which move eastwards. They have to be seen in conjunction with westward-moving terms of the same degree, but positive order because their superposition yields standing waves of the stated dual origin. Partial sums of zero order contribute to the Universal-time part of daily variations, together with the standing-wave parts of all other terms (see Appendix C in Part II). Their first terms of degree $n = 0$ are omitted because any arbitrary constant can be added to U, and a constant Z on $R = R$ can also be ignored. Consequently, if with $L \geq p$ the partial sums I_0 and J_0 are

included into the series, the total number of terms is one less than inferred from eq. (5).

Since Z must be derivable from the same potential U as X and Y, a relationship can be formulated between the expansion coefficients of both series. The required differentiation of U with respect to r on $r = R$ makes it now necessary to distinguish between parts of external and internal origin. For the potential coefficients of a given spherical term, the conventional notations are ϵ_n^m and $\imath_n^m$, respectively, and u_n^m is their sum. Within the range of validity of the potential concept, the external part has $(r/R)^n$ as r-dependence for all terms of degree n, and the internal part has $(R/r)^{n+1}$, to satisfy Laplace's equation $\nabla^2 U = 0$ and conditions at $r = 0$ and infinity. Differentiation of U term by term leads to the Gauss equations, connecting external and internal parts to the expansion coefficients of the two series:

$$\begin{aligned} u_n^m &= \epsilon_n^m + \imath_n^m \quad \text{(by definition)}, \\ z_n^m &= n\epsilon_n^m - (n+1)\imath_n^m \quad (\text{from } Z = \partial U/\partial r). \end{aligned} \tag{9}$$

Before closing this section with an outline of the least-squares analysis to derive coefficients from observations, a note may be appropriate on other formulations of the series. In Campbell's (1990) classification, the form of series expansions presented here follows Chapman's 'slice technique', but extended to allow longitude-dependent deviations from strict dependence on local time. This has also been Parkinson's (1977) approach. In other analyses, notably in those with Universal-time reference, coefficients are derived in pairs for westward- and eastward-moving waves, but Malin (1973) and Winch (1981) have demonstrated the relative smallness of the latter. Thus, in view of the limited number of terms that can be derived, it seems preferable to concentrate on those travelling westwards with the Sun. Appendix C gives the formulas to convert coefficients in real notation to complex notation, as used here.

Concerning the numerical execution of the spherical harmonic analysis, note that in using eqs (4) the series for U is converted into two series for the observables:

$$\begin{aligned} X_p &= I'_p + I'_{p+1}\,\mathrm{e}^{i\lambda} + I'_{p-1}\,\mathrm{e}^{-i\lambda} + I'_{p+2}\,\mathrm{e}^{i2\lambda} + I'_{p-2}\,\mathrm{e}^{-i2\lambda} + \ldots, \\ iY_p \sin\theta &= pI_p + (p+1)I_{p+1}\,\mathrm{e}^{i\lambda} + (p-1)I_{p-1}\,\mathrm{e}^{-i\lambda} + \ldots. \end{aligned} \tag{10}$$

As in eq. (7), common local-time factors on both sides are omitted and in the partial sums I'_m the derivatives $dP_n^m/d\theta$ replace P_n^m in eq. (8). Both series are used in conjunction and thus a data vector $\mathbf{y}$ of $2N$ components is formed with X_p and $iY_p \sin\theta$ from N observing sites. Similarly, a model vector $\mathbf{x}$ of M components represents the unknown expansion coefficients $u_n^m(p)$ to be found from observations. The multiplication of Y by $i \sin\vartheta$ is a computational convenience.

The least-squares problem is formulated for the data points at the actual position of the observatories involved, rather than for a mesh of equally spaced grid points, in order to avoid interpolation. If then the components of the model vectors are in sets of K coefficients of orders $m = p$, $m = p+1$, $m = p-1 \ldots$, then the rows of the connecting data kernel matrix $\mathbf{G}$ of dimension $(2N \times M)$ are filled with the spherical functions in the same sequence, using eqs (10) for U and eq. (7) for Z. For a given time harmonic, the (complex) elements of this matrix are solely determined by the coordinates of the observing sites, and the linear system to be solved is $\mathbf{Gx} = \mathbf{y} + \delta y$ with δy as the residual vector. Assuming $2N > M$, its least-squares solution for minimization of the squared residual norm is $\mathbf{x} = \mathbf{Hy}$, with

$$\mathbf{H} = (\mathbf{G}^{\mathrm{T}}\mathbf{G})^{-1}\mathbf{G}^{\mathrm{T}}, \tag{11}$$

where T denotes the adjoint matrix. A corresponding linear system applies to the expansion coefficients z_n^m with Fourier amplitudes Z_p as data, but now only N data are available to determine M coefficients.

With, say, $M = 12$ coefficients and almost a hundred observing sites one would expect the linear problem to have a stable least-squares solution. The very uneven distribution of sites, however, leads to numerical instabilities. These will be the main concern of Section 7. Since it is the purpose of this analysis to investigate term-by-term relationships, an unconstrained least-squares solution as formulated in eq. (11) is preferable, even though it limits the number of terms.

Stabilized solutions, either with Marquardt's method (Olsen 1991) or Tiknonov's regularization (Schultz & Zang 1994), are possible and thus permit the desirable inclusion of more terms. However they impose restrictive assumptions on the intended use of coefficients because they smooth over coefficients of different order and degree. It has been decided to avoid this additional complication and instead to restrict the number of terms.

5 THE SELECTION OF DAYS

Since it is intended to analyse daily variations under magnetic quiet conditions, the selection of suitable days will be based on the degree of global magnetic activity. A linear measure of this activity, within time intervals of three hours, is the *ap* index. For visualization, it can be associated with the peak-to-peak amplitude of symbolic oscillations in this interval, in units of 2 nT.

Following the example of Malin (1973) and Winch (1981), the five most disturbed days of each month, that is the international D-days, are excluded beforehand. From the remaining days in the two years of the IQSY, three data sets are formed. The first set, with 611 days, contains all days except the 120 D-days; the second set contains the five quiet international Q-days of each month and thus has 120 days. The third set includes quiet days in a new definition introduced here, based on a *fixed* upper limit for a specified sum of *ap* indices. This sum contains not only the eight indices of the considered day, but also the eight indices of the twelve hours before and after.

The reasons for requiring quietness on the adjacent half-days were stated in Section 3. If the sum of all sixteen *ap* indices does not exceed 60, the day is declared as quiet and termed a Q*-day. With the tolerated symbolic peak-to-peak amplitude of $60/16{\cdot}2 = 7.5$ nT in the average, the third data set comprises 124 Q*-days and thus is of comparable size to the second set. Naturally, there is a large overlap between the new Q*- and the old Q-days, but with notable exceptions. The month of August 1965 was one of continuous activity, and not a single day qualified as a Q*-day. In contrast, the month of December 1964 had such long-lasting quietness that six Q*-days could be added to the five Q-days of the month, thus exploiting this unusual condition more effectively. Table 2 gives the dates of Q*-days, month by month.

Further analysis of the three data sets has been conducted

Table 2. Q*-days during the IQSY.

Month	1964	1965
1	14 21 22	5 6 19 24 25 26 31
2	19	1 2 17 18
3	2 18 19 27 28	8 9 10 11 18 19
4	23	2 3 16 28
5	7 8 9 12 20	1 2 3 11 12 13 14 18 19 20 30 31
6	4 5 6 17	13 19 20 21 22 23 24
7	1 14 15 27	11 17 31
8	24	--
9	12 13 14 15 19 20 26	9 10 30
10	23 30 31	4 6 10 15 16 17 19 20 21
11	7 14 19 20 21 25	9 10 11 15 16 23 24 27 28 29
12	5 6 10 11 12 23 24 27 28 30 31	6 7 8 14 15 16 17 31

in two alternative ways, with *mean monthly daily variations* and with *daily variations on single days*. In the first case, the hourly values are averaged over the selected days of the month, hour by hour from midnight to midnight. In some cases too many data were missing, and mean monthly daily variations could not be formed. Such observatories are excluded for the entire year in order to have the same set of observing sites in all twelve months. For this reason three are left out in 1964 (LWI, MUT, LQA) and six in 1965 (LUA, LWI, PIL, VLA, HYB, VQC), leaving 74 (72) observatories for the 1964 analysis and 86 (84) observatories for the 1965 analysis. The numbers in parenthesis refer to the availability of Z. The observatory GUA has no Z for 1964, LQA has too many gaps in Z for 1965, and SFS has not reported Z at all.

It would have been impossible to proceed in a similar way in the analysis of single days. The gaps are spread so evenly over the year among the sites that no adequate set of observatories could have been assembled with data on *all* selected days of the year. In fact, this set would have consisted entirely of those 24 observatories with no gaps at all. Therefore it was decided to include on a given day all available data and thus to accept spherical harmonic analyses with slightly variable sets of observing sites from day to day. For example, of the 60 Q-days in 1964, 10 days have data from all 76 observatories in that year. On 40 days 74 to 75 observatories have data, and on 10 days only 71 to 74. These numbers are also representative for Q*-days and all days except D-days, with a comparable situation in 1965.

6 THE SELECTION OF OBSERVATORIES

It cannot be overlooked that the overall representation of the global *Sq* field by spherical harmonics is poor, for Z worse than for X and Y, even though jet regions with their spatial complexities have been excluded beforehand. Originally it was thought to reduce the effective number of observatories even further by attaching weights to them within an iterative process in accordance to the achieved fit. It turned out, however, that the observatory residuals, that is the differences between observed and synthesized time harmonics, are distributed in their real and imaginary parts so well in accordance with a normal Gaussian distribution that any weighting would have been unfounded. Only in two cases do excessive residuals occur, repeatedly on most days (or months) and generally in all harmonics, justifying a complete exclusion.

To illustrate these points, Fig. 2 shows for a very quiet day the first time harmonics as functions of latitude and in comparison to their approximations by spherical harmonics. Zero time reference as stated is local midnight. All observatories with data on that day are included. Since daily variations in X and Z are roughly symmetric about local noon (*cf*. Fig. 4), their cosine coefficients are displayed; for Y, which is antisymmetric about local noon, sine coefficients.

In spite of considerable scatter, the main characteristics of *Sq* are visible: in X, positive peak values at low latitudes, a change of sign at mid-latitudes and negative values at high latitudes. In Y the change of sign takes place slightly north of the equator. Clearly visible is the asymmetry of peak values at mid-latitudes. Because the selected day is already late in the year, the southern *Sq* vortex dominates, and thus the mid-latitude variations in Y are stronger here than in the northern hemisphere. In Z it is difficult to recognize any systematic latitude dependence. In northern latitudes cosine coefficients are consistently positive, as they should be, with just an indication of the expected reversal of sign at the equator.

It is therefore not surprising that on average over all sites spherical harmonics account for barely one-half of the amplitudes of the empirical time harmonics in the horizontal field and for one-quarter of them in Z, when four local-time terms are used. In Fig. 2 this is indicated by the scatter of data points around dashed theoretical curves, which show the dependences of the partial sums I'_p, and pI_p and J_p on latitude, for X_p, $i \sin\theta Y_p$, Z_p and $p = 1$, using their real or imaginary parts. For consistency, the least-squares fit also has been made with four local-time terms only.

In Z the poor fit can be attributed in all likelihood to ocean effects, in particular in the southern hemisphere, where most observatories are on either islands or coastlines. Notable exceptions are the observatories TSU in Namibia and PIL in Argentina. In the case of Australia, for example, opposing coast effects can be inferred directly from the identified Z coefficients for the two Australian observatories GNA and TOO. It is unclear to what extent induction anomalies, not connected to oceans, may contribute to the scatter in Z. Supporting evidence for this interpretation comes from the tendency of residuals to reoccur day after day in similar forms at many sites. Near to the equator, large residuals may reflect electrojet effects, in particular in the case of the first harmonic in X.

On the selected day the following rms residuals of U and Z were found with series expansions of four local-time terms

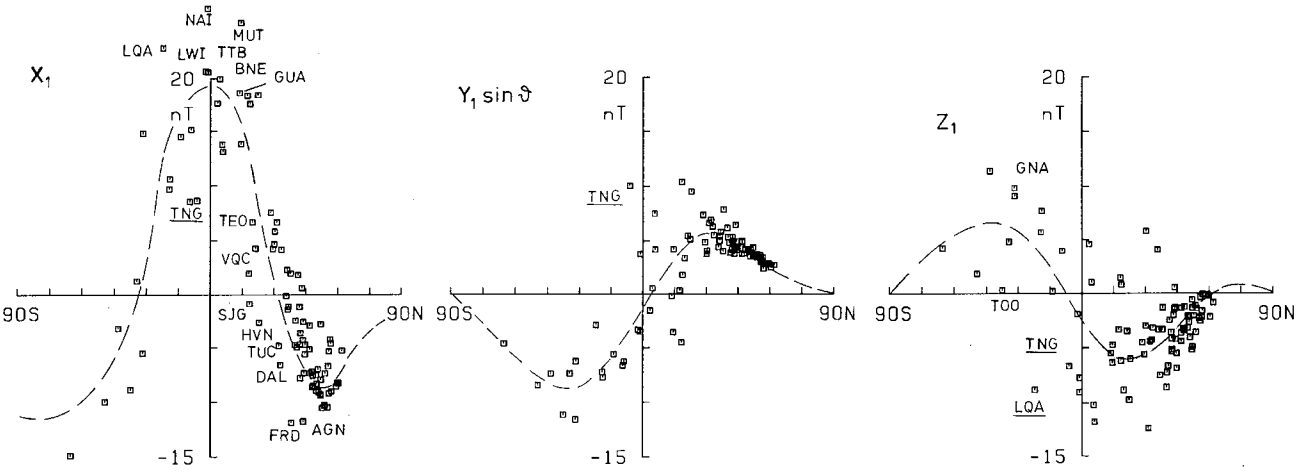

Figure 2. Daily variations on a very quiet day, 16 October 1965. The first time harmonics are shown as functions of geographical latitude for all 92 observatories with data on that day, either as cosine coefficients (X, Z) or as sine coefficients ($Y \sin\theta$). Zero time reference is local midnight. Signs are reversed for cosine coefficients to obtain positive peak values of X at low latitudes, corresponding to maximum upward deflections near local noon. Similarly, negative values of Z correspond to downward deflections at noon, and positive values of Y to upward deflections during morning hours as observed in the northern hemisphere (*cf*. Fig. 4). Dashed lines represent the theoretical latitude dependences from a least-squares fit with four spherical harmonics in local time. Deviations from equator symmetry (X, Z) or antisymmetry (Y) reflect the beginning of hemispherical imbalance of Sq source currents in late autumn. The harmonic coefficients displayed would be independent of longitude if daily variations were according to local time. That this is not strictly the case is evident from the marked observatories in Central and North America (TEO to AGN), which deviate clearly from the main cluster of the mostly European observatories for X. Also identified are observatories (LQA to GUA) with large X amplitudes. They are situated just outside the excluded equatorial electrojet region and are possibly still under some influence from the jet. The identified Australian observatories demonstrate opposite coastal effects for Z at the southwestern (GNA) and southeastern (TOO) corner of the continent. Two hereinafter excluded observatories (TNG, LQA) are underlined.

($L = 0$), in the notation of eq. (13):

$$\epsilon_U(1) = 3.42\ \text{nT}(6.36), \quad [2.63] \qquad \epsilon_Z(1) = 2.85\ \text{nT}(3.87), \quad [2.64]$$

$$\epsilon_U(2) = 2.45\ \text{nT}(4.87), \quad [1.98] \qquad \epsilon_Z(2) = 2.24\ \text{nT}(3.10), \quad [1.91]$$

Numbers in parentheses are rms amplitudes according to eq. (14), for comparison. Those in square brackets below are the rms residuals, when with $L = 1$ eight general terms are added. They improve the fit substantially, and suggest that the scatter of data points is partially due to changes of daily variations with longitude. By adding more general terms the fit can be improved further, but with 16 general terms for $L = 2$ the limits of numerical stability are reached, as shown later. In Fig. 2, longitude dependence is directly visible at the Central and North American observatories, which are identified in the diagram for X_1 by their names (TEO to AGN). All deviate systematically from the remaining, mostly Eurasian, observatories.

It could be argued that a similar display for daily variations in the average over a certain month or season would lead to more consistent results, but this is definitely not the case. The chosen day was anyhow of such exceptional quietness, with Kp indices of zero and $1-$, that virtually no substorm activity could be made responsible for the deviating data points. In order to strengthen this argument, Fig. 3 shows in the left-hand diagram coefficients for mean daily variations in October 1965, that is each data point now represents an average over nine quiet days of that month, with only little change in the degree of scatter. The idea that instead the neglected longitude dependence is largely responsible for the poor fit finds support in the central diagram of that figure. It displays Fourier coefficients for the same single quiet day as in Fig. 2, but corrected for longitude effects. It implies that after a spherical harmonic expansion with 12 terms, its eight general terms were synthesized and subtracted from the original Fourier coefficients, site by site. This correction clearly improves the fit to the dashed theoretical curve, at least at mid-latitudes.

The right-hand diagram of Fig. 3 repeats the display of Fourier coefficients for the quiet day of Fig. 2, but now with those observatories added that have so far been omitted because their geomagnetic latitude was considered too high or their dip latitude too low. For orientation in the changed scaling, the theoretical curve of Fig. 2 is included. As to be expected, strong and complicated results are obtained in both jet regions which justifies the exclusion of their data. An unrealistically large number of spherical terms would have been needed for an adequate fit at all latitudes.

A thorough examination revealed that a few observatories have the most excessive residuals on nearly all days and in all harmonics. They are also identified by underlined names in Fig. 2: TNG in Indonesia for all components, VQC in the Caribbean for X and Y, LQA in South America for Z. None of these data will be used. Their omission leads to an impressive reduction of rms residuals, even though only two observatories from almost 100, for a given component, are left out. For series approximations with 12 terms the potential residuals decline from 2.63 to 1.98 and from 1.98 to 1.54 for the first and second time harmonics. The corresponding reductions for Z are 2.64 to 2.38 and 1.91 to 1.61. These are generally valid results for expansions with the quoted number of terms. Hence, in the average over all sites and days, in the forthcoming analyses a 12 spherical harmonics can account for about two-thirds of the observed horizontal amplitudes and for about one-half of

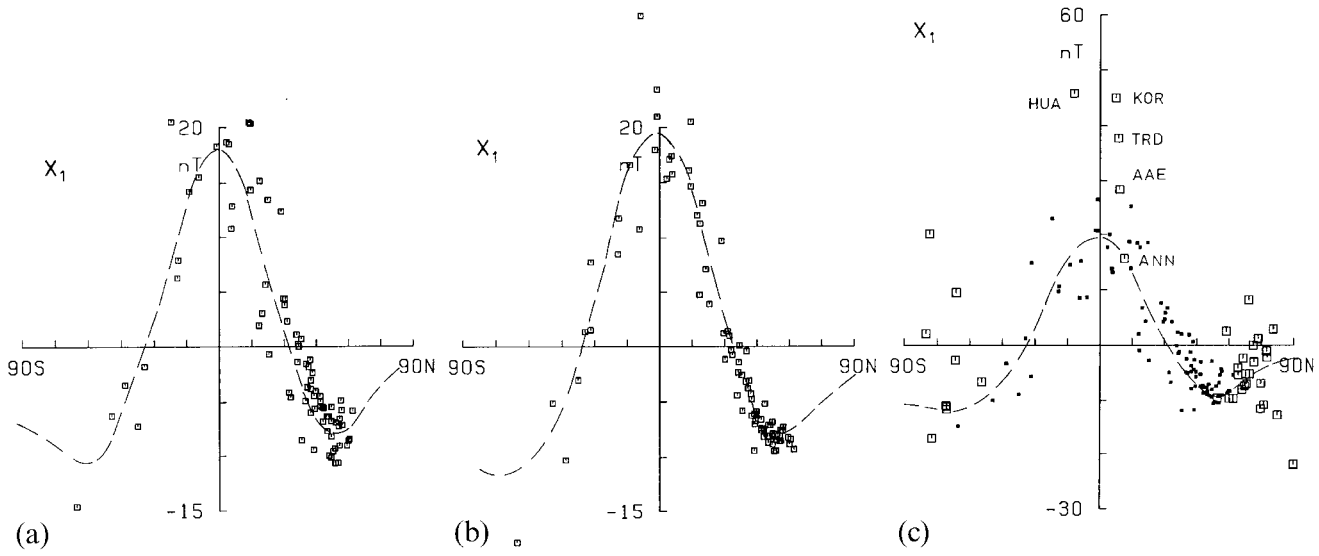

Figure 3. Negative cosine coefficients of the first time harmonic of daily variations in X, in the same presentation as in Fig. 2. (a) Coefficients of *mean* daily variations of nine quiet days in October 1965. They display a comparable degree of scatter to the single-day coefficients in Fig. 2. (b) *Single-day* coefficients of 16 October 1965, after corrections for dependence on longitude (see text). This improves the fit in mid-latitudes, but leaves scattered peak values near the equator unchanged, when compared to the corresponding diagram in Fig. 2. (c) *Single-day* coefficients of 16 October 1965, including the so-far omitted polar and equatorial observatories (identified by larger symbols). A twofold increase in the scaling factor is needed to accommodate the strongly enhanced harmonics under the equatorial electrojet (HUA to ANN), while scattered, but not everywhere excessive, values are found in the polar jet regions.

the observed vertical amplitudes. In summary, these are the final numbers of observatories to be used:

	1964	1965
monthly means:	73 (71)	85 (83)
single days:	$\leq$76 (75)	$\leq$90 (90)

Numbers in parenthesis refer again to the availability of Z.

Finally, Fig. 4 shows for a single quiet day, which once more is 16 October 1965, how well spherical and time harmonics can approximate observed daily variations in space and time. The twofold synthesis is carried out for representative sites at low and mid-latitudes, north and south of the equator. The original time series, in Universal time, are shown in the left-hand diagrams. Since the selected sites are at different longitudes, no consistent global picture of Sq variations can arise. In the centre the results are given for a time harmonic synthesis with six harmonics, yielding a slightly smoothed image of the original data. Because of the phase shift to local time, the typical Sq characteristics in late northern autumn emerge.

The time series on the right-hand side represent a combined spatial spherical harmonic and subsequent time harmonic synthesis. 12 spherical terms are used for each time harmonic. This reconstruction of the global time–space structure of daily variations reproduces the original data quite well at all sites and in most components. Exceptions are X in LGR, Y in GUA, and Z in PIL, where the synthesized variations do not quite reach the observed ones in amplitude. It should be added that *continental* observatories have been chosen for the southern hemisphere. Otherwise, much larger discrepancies in Z would have impaired the favourable impression of the achieved fit to the data.

7 THE SEARCH FOR AN OPTIMUM NUMBER OF SPHERICAL HARMONICS

A compromise has to be found between the desired closeness of fit and the numerical stability of the least-squares solution. To this end, a test series of spherical harmonic analyses has been conducted. The data are again the time harmonics of 16 October 1965, but it has been ascertained that the conclusions drawn are generally valid for days of comparable quietness. $K = 4$ terms are chosen for all the partial sums in the series for U and Z, while the number of general terms increases from zero for $L = 0$ to 32 for $L = 4$.

The use of four local-time terms is an absolute minimum. The first and third terms of order p and degrees $n = p$ and $n = p + 2$ are associated with spherical functions, which are symmetric with respect to the equator and thereby indispensable for expressing the hemispherical imbalance of Sq during summer and winter. Furthermore, besides the clearly required principal second term with $n = p + 1$, one additional anti-symmetric term with $n = p + 3$ is needed because of source-field considerations. A review of such a requirement can be found in Winch's treatise (1981; p. 37). The significance of this fourth term is evident from its relative prominence in the amplitude spectra of local-time coefficients in Fig. 5, at least up to the third harmonic.

These spectra also show that general terms are of comparable size and essential for accounting for the longitude dependence of daily variations, as clearly demonstrated in the previous section. There are no signs of convergence in the spectra, which towards higher harmonics appear more and more as 'white'. This holds when with $L = 4$ up to 32 general terms are included. Hence, the necessary truncation of the series is arbitrary and will be guided by stability considerations. Even though strict

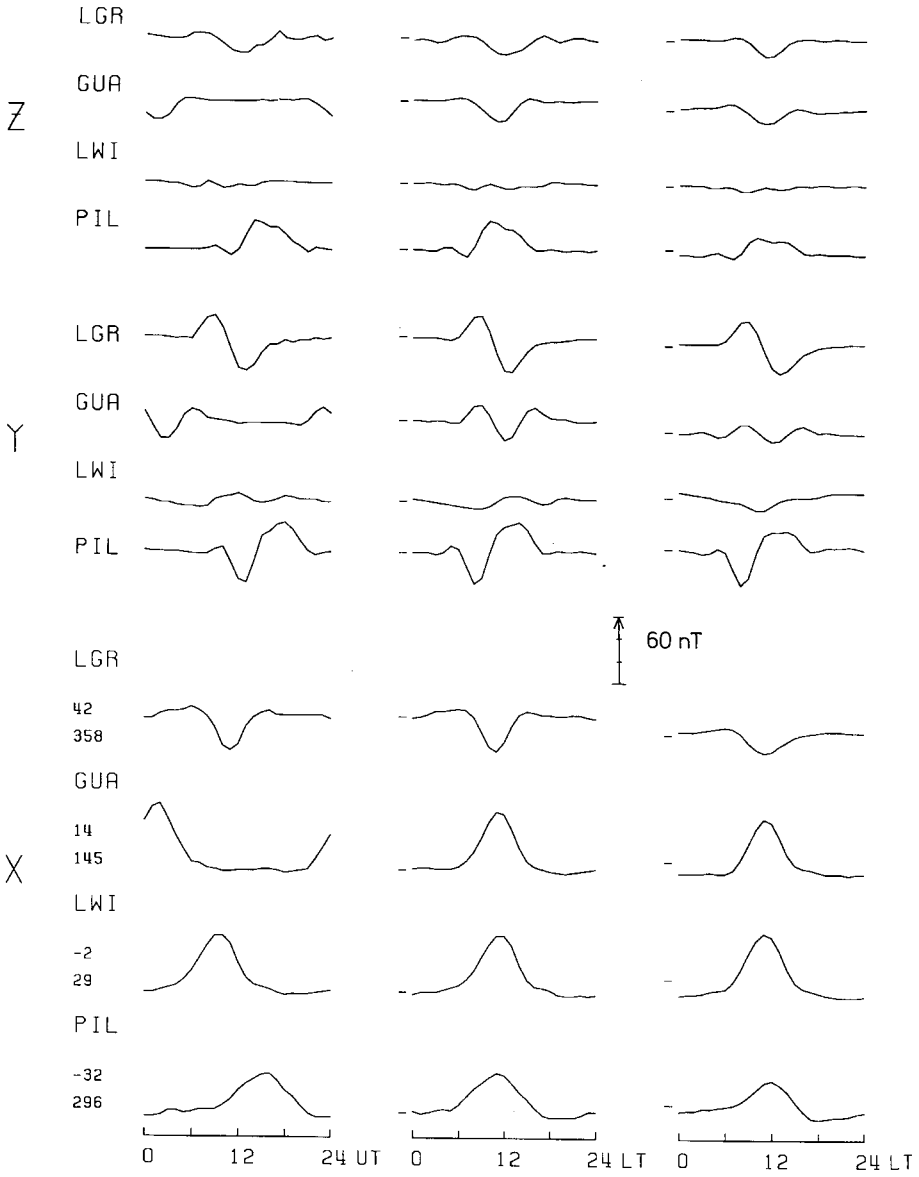

Figure 4. Synthesis of daily variations on a very quiet day at four representative sites at mid- and low latitudes, in both hemispheres. Geographical coordinates are below the last set of observatory acronyms. (Left) Original hourly means on the chosen Greenwich day, 16 October 1965, in Universal time UT. (Centre) Hourly means from a time harmonic synthesis with the six harmonics of that day, phase-shifted to local midnight and including absolute terms, in local time LT. (Right) Hourly means from a combined spherical and time harmonic synthesis, using 12 spherical terms to synthesize each of the six time harmonics. Dashes indicate the zero reference level of the synthesized daily variations. It is identical with the local midnight level in the time harmonic synthesis but deviates slightly from that level, for X and Z, in the combined synthesis, due to internal currents across the midnight meridians (see Appendix A and Fig. 6 of Part II, lower right).

orthogonality is lost by the use of spherical harmonics with discrete dependences on co-latitude, the influence of the chosen truncation level is not very strong, at least not within the limits set by numerical stability. Table 3 shows results for the principal term of the second time harmonic, when the number of terms is varied between $M = 1$ and $M = 35$. The first entry is for an analysis with the principal term only. It seems that beyond $M = 12$, that is for more than eight general terms, numerical instability begins, in the expansion of Z more so than for the potential, a notion which will find further support in the course of this section.

In order to express the closeness of the achieved overall fit by a single number, rms residuals ϵ are introduced, in the average over all observatories at a fixed frequency. For the kth observatory of a total of N, and the pth time harmonic,

$$\Delta F_{pk} = F_{pk}^{\mathrm{obs}} - F_{pk}^{\mathrm{syn}}, \tag{12}$$

defines the individual observatory residual, with F standing for X, $i \sin\theta Y$, or Z. The superscripts 'obs' and 'syn' identify observed and synthesized time harmonics. The rms residuals are then

$$\epsilon_U(p) = \left\{ \frac{1}{N} \sum_k \left[|\Delta X_{pk}|^2 + \sin^2\theta_k |\Delta Y_{pk}|^2 \right] \right\}^{1/2},$$
$$\epsilon_Z(p) = \left\{ \frac{1}{N} \sum_k |\Delta Z_{pk}|^2 \right\}^{1/2} \tag{13}$$

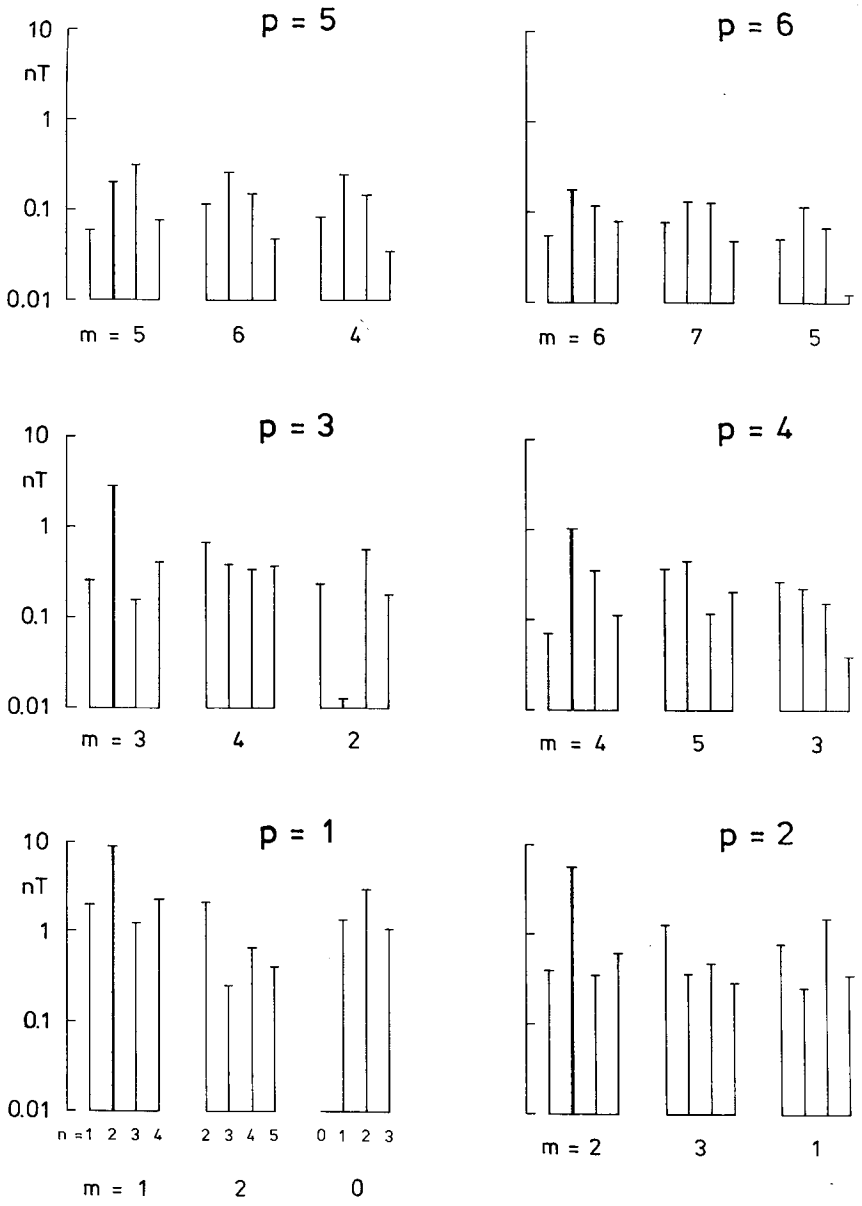

Figure 5. Spherical harmonics of daily variations on a very quiet day, 16 October 1965. Vertical bars represent moduli of the 12 potential coefficients $u_n^m(p)$ for each of the six time harmonics $p=1$ to $p=6$. They are arranged in three groups: four local-time terms of orders $m=p$ and eight general terms of orders $m=p\pm1$. In each group degrees increase from $n=m$ to $n=m+3$. The second local-time terms with $n=p+1$ are marked by heavy lines. They dominate as 'principal terms' the spectra up to the fourth harmonic, which otherwise are without structure and in particular without signs of convergence. The featureless spectra for the fifth and sixth harmonics assign them to the background spectrum of irregular variations. See also Figs 3 and 4 of Part II for the day-to-day and seasonal variability of separated external and internal potential coefficients.

Table 3. Coefficients of the principal spherical harmonic term for the potential and the vertical component, in nT. Series expansions refer to the second time harmonic of daily variations on 16 October 1965, with varying numbers M of spherical terms.

M	1 (L=0)	4 (0)	12 (1)	19 (2)	35 (4)
$u_3^2(2)$	- 4.71 - 2.65 i	- 4.75 - 2.43 i	- 4.84 - 2.50 i	- 4.66 - 2.28 i	- 4.33 - 1.84 i
$z_3^2(2)$	- 5.04 - 0.51 i	- 5.95 + 0.11 i	- 5.19 + 0.14 i	- 4.06 + 1.12 i	- 1.87 + 4.48 i

for the series in U and Z, respectively. Their squares multiplied by N represent the minimized sums by the least-squares procedure.

Table 4 illustrates how an increasing number of terms gradually reduces rms residuals. In its first row again are the results of a single-term analysis with the principal term only. As to be expected for this day, almost one month after autumnal equinox, a substantial improvement of the fit takes place when four local-time terms instead of one are used. Also, the inclusion of the first eight general terms has a marked effect, even though the improvements achieved are unevenly distributed among observatories, as was clear already from the central diagram of Fig. 3. Further reductions of residuals are possible, but instabilities with oscillating solutions start well before the 'degrees of freedom', $2N - M$ for U and $N - M$ for Z, come even close to zero, noting that data from $N = 90$ observatories are available.

To allow an estimation of the residuals in relation to the observed time harmonics, rms amplitudes

$$a_U(p) = \left\{ \frac{1}{N} \sum_k |X_{pk}^{\mathrm{obs}}|^2 + \sin^2 \theta_k |Y_{pk}^{\mathrm{obs}}|^2 \right\}^{1/2}, \qquad a_Z(p) = \left\{ \frac{1}{N} \sum_k |Z_{pk}^{\mathrm{obs}}|^2 \right\}^{1/2} \tag{14}$$

are listed in the bottom row of Table 4. Numbers in parenthesis are the model norms $|x|$ in the notation of eq. (11). Their steep increase for Z beyond $M = 20$ once again signals the beginning of instability with oscillating solutions, but no comparable increase is visible for the norm of potential coefficients up to $M = 36$. This would imply an achievable relative fit in X and Y of 80 per cent with 36 terms and in Z of 50 per cent with 20 terms. These projections are, however, too optimistic, as will be seen.

No attempt is made to assign confidence limits to the coefficients. Malin (1973, p. 572) defines standard deviations for them, which he derives from the squared residuals ϵ^2, divided by the quoted degrees of freedom and multiplied by the diagonal element h_{kk} in the solution matrix $\mathbf{H}$ of eq. (11). In fact, the sum of squared elements in one row of $\mathbf{H}$ would provide a direct measure of individual model variances, if all data had the same rms errors and if errors were *independent* random variables. In particular, the second condition may be violated and a substantial mutual dependence of errors at neighbouring sites would require the use of a fully occupied covariance matrix of errors.

Even though rising coefficient variances would be the best indicators for the onset of instability, it was felt that the required estimates of data errors are poorly founded. As a substitute, a data-independent measure will be used by deriving the (real) eigenvalues λ^* for the eigenvalue problem $\mathbf{G}^{\mathrm{T}}\mathbf{G}\mathbf{u} = \lambda^*\mathbf{u}$ where $\mathbf{u}$ denotes eigenvectors and $\mathbf{G}^{\mathrm{T}}\mathbf{G}$ is the normal equation matrix of the least-squares solution in eq. (11). If the range of eigenvalues is very large, extending over orders of magnitude, certain linear combinations of expansion coefficients will be practically indeterminable from the data. For a test of stability, only the *condition number*, that is the ratio of the largest to the smallest eigenvalue, needs to be considered. Table 5 lists them for the same ascending number of terms as in Table 4. The single-term analysis, which does not require a matrix inversion, is left out. The entries are for the second time harmonic, but the condition numbers for the other harmonics are similar because the elements of $\mathbf{G}$ are

Table 4. Spherical harmonic analysis of daily variations on 16 October 1965, with 90 observatories. Listed are rms residuals $\epsilon(p)$ according to eq. (13) for a least-squares fit with series expansions containing an ascending number M of spherical harmonic terms, for time harmonics $p = 1$ to $p = 4$. If the series parameter $L \geq p$, then the number of terms is one less. The model vector norm $|x|$ of expansion coefficients is below the residuals in parentheses. The bottom row rms lists amplitudes $a(p)$ according to eq. (14) to illustrate the relative size of residuals. All entries are in units of nT.

	Potential U				Vertical component Z			
p	1	2	3	4	1	2	3	4
M = 1	3.90	2.29	1.99	1.14	2.91	2.02	1.40	0.91
(L = 0)	(8.47)	(5.40)	(3.02)	(1.19)	(4.48)	(5.07)	(4.23)	(2.47)
M = 4	2.96	2.14	1.42	1.03	2.60	1.93	1.35	0.82
(0)	(9.23)	(5.40)	(2.88)	(1.04)	(7.11)	(6.25)	(4.40)	(2.22)
M = 12	1.98	1.54	1.19	0.89	2.38	1.61	1.12	0.72
(1)	(9.88)	(5.98)	(3.18)	(1.30)	(8.16)	(7.56)	(5.75)	(2.95)
M = 20	1.81	1.33	0.98	0.71	2.19	1.49	1.00	0.64
(2)	(10.07)	(5.99)	(3.17)	(1.38)	(10.3)	(9.01)	(7.14)	(3.49)
M = 28	1.46	1.09	0.88	0.66	1.75	1.14	0.85	0.55
(3)	(9.97)	(5.88)	(3.15)	(1.58)	(26.1)	(24.2)	(13.6)	(13.0)
M = 36	1.25	1.01	0.80	0.59	1.34	1.02	0.77	0.50
(4)	(10.6)	(5.94)	(3.32)	(1.70)	(75.5)	(48.2)	(42.6)	(13.2)
a(p)	6.28	4.87	3.19	1.67	3.74	2.96	2.05	1.17

Table 5. Condition numbers of the normal equation matrix $\mathbf{G}^T\mathbf{G}$ in eq. (11) for ascending numbers M of spherical harmonic terms in the two series expansions. Least-squares fit for the second time harmonic with data from N magnetic observatories. If variable observatory weights are used, their effective number follows below in parentheses. Column 1: all 90 observatories with data in 1965; column 2: 74 northern hemisphere observatories only; column 3: balanced set of 55 northern and southern hemisphere observatories; columns 4 and 5: all 90 observatories again, but with variable weights (see text).

	Potential U					Vertical component Z				
N	90	74	55	90 (60.5)	90 (34.5)	90	74	55	90 (60.5)	90 (34.5)
M = 4	7.8	399	4.3	3.6	4.5	11.8	9118	5.7	4.6	5.5
12	30.8	5705	17.1	12.5	23.2	62.6	$>10^4$	26.3	18.9	30.2
19	85.2	$>10^4$	40.3	29.1	40.8	288		115	89.5	101
27	180		79.2	57.0	87.8	5942		2517	1878	3321
35	388		167	120	208	$>10^4$		$>10^4$	$>10^4$	$>10^4$

mainly dependent on the number and coordinates of observation points. The reservation is necessary again because different sets of spherical harmonics are used for different time harmonics. Since individual coefficients without smoothing are needed, the initiated singular value decomposition will not be used for stabilizing the solution.

The first columns of Table 5 contain the eigenvalue ratios, when least-squares solutions are sought with data from all 90 observatories available for 1965. Accepting ratios of up to 100 for stable estimates, the spherical harmonic expansion of Z should not go beyond the inclusion of 12 terms. Obviously, more could be used in the expansion of U because two horizontal field components are involved. It was decided, however, to adopt for both series $M = 12$ terms with series parameters $K = 4$ and $L = 1$, for clarity. All further analyses are carried out in this way unless stated otherwise. It is noteworthy that Parkinson (1977) used exactly the same number of terms, i.e. 24 terms in his real notation, while Malin (1973) included up to 36 and Winch (1981) up to 40 terms.

The remaining columns of Table 5 show the results of a numerical experiment. The eigenvalue ratios in the second columns refer to an analysis without the 16 sites in the southern hemisphere and thus with 74 sites in northern latitudes only. The results are disastrous. It is hardly possible to go beyond a single-term analysis. For entries in the third columns, the omitted sites are included again and 35 sites in the northern hemisphere are left out, with the distribution of remaining 39 sites as even as possible. This more balanced network of 55 observing points not only restores stability, but even improves it well above the level with all 90 sites. The conclusions are twofold: (1) southern hemisphere observatories are indispensable, unfavourable as their locations may be on islands and coastlines; (2) none of the northern hemisphere observatories is superfluous, but they should not enter with the same weight into the least-squares solution.

Therefore all 16 observatories in the southern hemisphere and 15 isolated observatories in the northern hemisphere now receive full weights, while the remaining 59 more closely spaced sites north of the equator enter with half weights. Numerically this implies that their time harmonics and the elements in the corresponding row of matrix $\mathbf{G}$ are divided by two. Altogether, the effective number of observatories now amounts to $16 + 15 + 59/2 = 60.5$. The resulting new eigenvalue ratios can be found in the fourth columns of Table 5. They reveal most clearly that this form of weighting leads to an increase of stability, and further experiments with weights have shown that these results are the best that can be achieved. The entries in the fifth and last columns demonstrate, for example, that a complete hemispherical balance, obtained with one-quarter weights for all 74 observatories in northern latitudes, undervalues the potential which these sites have for an optimum solution, in spite of their close spacing.

Hence, in all forthcoming analyses, full and half observatory weights are used according to the entries in the last column of Table 1. The resulting effective numbers of observatories are $13 + 11 + 52/2 = 50$ for 1964, and the already cited 60.5 for 1965, provided that no data are missing. It is noteworthy again that Parkinson (1977, p. 15) anticipated the adverse effects of a similar hemispherical imbalance during the IGY and excluded many observatories in northern latitudes available to him.

Table 6. Condition numbers of normal equation matrix $\mathbf{G}^T\mathbf{G}$ in eq. (11) as in Table 5, but assuming data from N fictitious sites in an evenly spaced network of stations.

	Potential U			Vertical component Z		
N mesh [1]	90 18 x 36	56 22 1/2 x 45	30 30 x 60	90 18 x 36	56 22 1/2 x 45	30 30 x 60
M = 4	2.5	2.5	2.5	1.8	1.8	1.8
12	4.6	4.7	6.9	4.1	4.1	6.3
19	9.6	9.6	12.5	5.0	5.0	15.5
27	10.7	11.2	16.3	5.8	6.2	$>10^4$
35	11.9	13.3	19.6	6.6	$>10^4$	--

[1] in degrees latitude × longitude

This section closes by considering the hypothetical possibilities which an evenly spaced network of observatories could provide. All calculations are repeated and the resulting eigenvalue ratios can be found in Table 6. The entries in the first columns are for nine sites along meridians, leaving out the poles, and 10 sites along circles of latitude, which yields a $18^\circ \times 36^\circ$ mesh of $N = 90$ fictitious points of observation. Their even distribution reduces the range of eigenvalues dramatically, making it simple to calculate 36 spherical terms in both series. The entries in the next columns refer to the more coarse distributions of a $22.5^\circ \times 45^\circ$ mesh with $N = 56$ and of a $30^\circ \times 60^\circ$ mesh with $N = 30$ sites, respectively. Even for these reduced numbers of sites, stable determinations remain possible, with eigenvalue ratios well below those found for optimum weighting for the network of observatories during the IQSY.

The conclusion is that a temporary installation of not too many additional magnetometer stations, at crucial sites to create a better balanced network, would allow a greatly improved spherical harmonic analysis. With the existing network a few quiet days with simultaneous records are sufficient, as will be demonstrated in Part II (Schmucker 1999). This second part will close with a critical review of all obtained results, prospects for their improvement and augmentation, and with acknowledgments.

REFERENCES

Ashour, A.A. & Price, A.T., 1965. Night-time earth currents associated with the daily magnetic variations, *Geophys. J.,* **10,** 1–15.

Campbell, W.H., 1990. Differences in geomagnetic Sq field representations due to variations in spherical harmonic analysis techniques, *J. geophys. Res.,* **95,** 20 923–20 936.

Chapman, S., 1919. The solar and lunar diurnal variation of the earth's magnetism, *Phil. Trans. R. Soc. Lond.* A, **218,** 1–188.

Chapman, S. & Bartels, J., 1940. Geomagnetism, Clarendon Press, Oxford.

Haines, G.V. & Torta, J.M., 1994. Determination of equivalent current sources from spherical cap harmonic models of geomagnetic field variations, *Geophys. J. Int.,* **118,** 499–514.

Kuvshinov, A.V., Avdeev, D.B. & Pankratov, O.N., 1999. Global induction by Sq and Dst sources in the presence of oceans: bimodal solution for non-uniform spherical surface shells above radially symmetric Earth models in comparison to observations, *Geophys. J. Int.,* submitted.

Malin, S.R.C., 1973. Worldwide distribution of geomagnetic tides, *Phil. Trans. R. Soc. Lond.,* **274,** 551–594.

Olsen, N., 1991. Untersuchungen von tagesperiodischen Variationen des Erdmagnetfeldes mit neueren statistischen Methoden, *PhD thesis, University of Goettingen.*

Parkinson, W.D., 1977. An analysis of the geomagnetic diurnal variations during the International Geophysical Year, *Bulletin 173,* Australian Government Publ. Service, Canberra.

Price, A.T. & Stone, D.J., 1964. The quiet-day magnetic variations during the IGY, *Ann. IGY,* **35,** 63–269.

Price, A.T. & Wilkins, G.A., 1963. New methods for the analysis of geomagnetic fields and their application to the Sq field of 1932–3, *Phil. Trans. R. Soc. Lond.,* **256,** 31–98.

Rikitake, T., 1950. Electromagnetic Induction within the Earth and its relation to the electrical state of the Earth's interior, *Bull. Earthq. Res. Inst. (Tokyo Univ.),* **28,** 45–100, 219–262, 263–283.

Schmucker, U., 1999. A spherical harmonic analysis of solar daily variations in the years 1964–1965: response estimates and source fields for global induction—II. Results, *Geophys. J. Int.,* **136,** 455–476 (this issue).

Schultz, A. & Zhang, T.S., 1994. Regularized spherical harmonic analysis and 3-D electromagnetic response of the Earth, *Geophys. J. Int.,* **116,** 141–156.

Schuster, A., 1889. The diurnal variation of terrestrial magnetism, *Phil. Trans. R. Soc. Lond.,* A, **180,** 467–518.

Torta, J.M. & DeSantis, A.D., 1996. On the derivation of the Earth's conductivity structure by means of a spherical cap harmonic analysis, *Geophys. J. Int.,* **127,** 441–451.

Winch, D.E., 1981. Spherical harmonic analysis of geomagnetic tides, 1964–65, *Phil. Trans. R. Soc. Lond.,* **303,** 1–104.

APPENDIX A: THE TRUE ZERO BASELINE

Ideally, daily variations should be measured from a baseline, which the undisturbed geomagnetic field provides, after a hypothetical removal of all transient variations of external and internal origin. This 'true zero' baseline, however, is not accessible to direct observation, and, as a substitute, the local midnight field level is commonly used, as has been done in this study. On quiet days and after the removal of still existing *Dst* fields, this level may be close to true zero, but only when the midnight level coincides with the daily mean. Otherwise, as first pointed out by Price & Stone (1964), problems arise from the presence of substantial internal currents during the night hours, crossing the midnight meridian, and we have to distinguish between *observable* daily means X_0, Y_0, Z_0, measured from the midnight levels, and *desired* daily means X_0', Y_0', Z_0' from the unknown true zero baselines X_{00}, Y_{00}, Z_{00} of the Earth's quasi-permanent field. Denoting in the case of X the daily mean of the total field $X(T)$ with $\bar{X}$, in local time T, then $X_0 = \bar{X} - X(0)$ and $X_0' = \bar{X} - X_{00}$, which gives in $X_0 - X_0' = X_{00} - X(0)$ the offset of true zero against the local midnight level.

For daily variations in Y, which are antisymmetric with respect to local noon, the daily mean $\bar{Y}$ will be close to the midnight level and Y_0 will more or less agree with Y_0'. This is not so, however, in the case of X and Z. Their means will be widely separated from the midnight level, as evident from Fig. 4, and a reduction to the true zero baselines will be essential for an adequate display of equivalent external and internal induced currents. The stated possibility of night-time internal fields, even in the total absence of external fields, arises from the fact that, for induction, only deviations from a time-constant level matter, here the daily mean of the total field, after the removal of the non-cyclic change on that day.

An example may illustrate this point, in which for simplicity a single harmonic oscillation in local time is used to represent external daily variations in X. Measured from true zero and with T in angular measure,

$$X_{\text{ext}}(T) = A(1 - \cos T), \tag{A1}$$

which with $A > 0$ may resemble for $T = \pi$ the noon peak in X at low latitudes. Induced daily variations arise from the *transient* part of X_{ext} only, and are superimposed on the quasi-permanent field of likewise internal origin. By approximating the external source by a single spherical harmonic, with Q as its complex-valued internal to external potential ratio for the fundamental period,

$$X_{\text{int}}(T) = X_{00} - A|Q| \cos(T + \alpha), \tag{A2}$$

with $\alpha = \arg\{Q\}$. Hence, the total field $X(T)$, as the sum of external and internal fields, has the daily mean $\bar{X} = A + X_{00}$ of dual origin and is below true zero at local midnight, when $X(0) = X_{00} - A|Q| \cos\alpha$. With a noon peak of, say, $2A = 60$ nT

and an in-phase Q-ratio of 0.4, the offset amounts to a quite significant 12 nT. As a consequence, the observable daily mean from the midnight level is increased by induction from $X'_0 = A$ to $X_0 = A(1 + |Q| \cos \alpha)$; that is, from 30 nT above true zero to 42 nT above the midnight level. For more detailed calculations the reader is referred to Ashour & Price (1965).

Any assumption-free derivation of the baselines would require a global separation analysis of the daily means of the total field, yielding in their internal part the desired true zero baselines. However, it is possible to reconstruct these baselines from the observable daily means directly, without recourse to the problematic separation of the total field, which is dominated by the Earth's quasi-permanent field. The only necessary supposition is that fields of external origin are everywhere zero at local midnight, as in the example. Otherwise there would be an undetectable time-constant field of external origin. If the stated supposition holds, however, then the offset between the midnight level and true zero is *exclusively internal*, while daily means from any level are always *exclusively external*. Since the observable daily means are the sums of these offsets and the daily means from true zero, a spherical harmonic analysis of X_0, Y_0, Z_0 and their subsequent separation yields in the external parts the desired daily means X'_0, Y'_0, Z'_0 against true zero, and, after their subtraction from $\bar{X}, \bar{Y}, \bar{Z}$, the true zero baselines themselves.

APPENDIX B: ON SERIES WITH SPHERICAL HARMONICS

Depending on the sequence of summations, infinite series for the potential of the pth time harmonic can be written in two alternative forms, using complex notation:

$$U_p = \sum_{n=1}^{\infty} \sum_{m=-n}^{+n} u_n^m P_n^m(\cos\theta)\, \mathrm{e}^{im\lambda}$$

or

$$U_p = \sum_{m=-\infty}^{+\infty} \mathrm{e}^{im\lambda} \sum_{n=|m|}^{\infty} u_n^m P_n^m(\cos\theta). \tag{B1}$$

If $m = 0$, then the term with $n = 0$ is omitted. In the second form the truncation of the series requires first a specified range of orders m and second a specified maximum degree n, for a given order. In the analysis of daily variations performed here, a symmetric range is chosen with respect to order $m = p$, and the same number K of spherical harmonic terms of ascending degree is included for all orders:

$$U_p = \mathrm{e}^{ip\lambda} \sum_{m=p-L}^{p+L} \mathrm{e}^{i(m-p)\lambda} \sum_{n=|m|}^{|m|+K-1} u_n^m P_n^m(\cos\theta). \tag{B2}$$

Series parameter $K = 1, 2, \ldots$ and $L = 0, 1, 2, \ldots$ are the same for all harmonics. The longitude factor $\exp(ip\lambda)$ has been separated to allow its combination with the Universal-time factor $\exp(ipt)$ to form, with $T = t + \lambda$, the local-time factor $\exp(ipT)$.

APPENDIX C: SPHERICAL HARMONICS IN REAL AND COMPLEX NOTATION

For a spherical harmonic of degree n and order m, Malin (1973) denotes by g_n^m and h_n^m real-valued unseparated potential coefficients, which are associated with the longitude factors $\cos m\lambda$ and $\sin m\lambda$, respectively. He adds either a_p or b_p in parentheses to identify their connection to cosine or sine coefficients of the pth time harmonic, in Universal time. Similarly, complex potential coefficients u_n^m and u_n^{-m} are connected to $\exp(im\lambda)$ and $\exp(-im\lambda)$, respectively, with a common time factor $\exp(ipt)$. This establishes for $m \neq 0$ the identity

$$\begin{aligned}&[g_n^m(a_p)\cos m\lambda + h_n^m(a_p)\sin m\lambda]\cos pt \\ &\quad + [g_n^m(b_p)\cos m\lambda + h_n^m(b_p)\sin m\lambda]\sin pt \\ &= \mathscr{R}e\{[u_n^m\, \mathrm{e}^{im\lambda} + u_n^{-m}\, \mathrm{e}^{-im\lambda}]\, \mathrm{e}^{ipt}\},\end{aligned} \tag{C1}$$

from which it follows that

$$\begin{aligned}u_n^m &= \frac{1}{2}\{[g_n^m(a_p) - h_n^m(b_p)] - i[h_n^m(a_p) + g_n^m(b_p)]\}, \\ u_n^{-m} &= \frac{1}{2}\{[g_n^m(a_p) + h_n^m(b_p)] + i[h_n^m(a_p) - g_n^m(b_p)]\}.\end{aligned} \tag{C2}$$

Conversely, if both u_n^m and u_n^{-m} are available, which in this study is not usually the case, then

$$\begin{aligned}g_n^m(a_p) &= \mathscr{R}e\{u_n^{-m} + u_n^m\}, \qquad g_n^m(b_p) = -\mathscr{I}m\{u_n^{-m} + u_n^m\}, \\ h_n^m(a_p) &= \mathscr{I}m\{u_n^{-m} - u_n^m\}, \qquad h_n^m(b_p) = \mathscr{R}e\{u_n^{-m} - u_n^m\}.\end{aligned} \tag{C3}$$

For terms of order $m = 0$,

$$u_n^0 = g_n^0(a_p) - ig_n^0(b_p). \tag{C4}$$

Malin's analysis does not include series expansions of absolute terms.

Parkinson (1977) and Winch (1981) also derive coefficients in real notation. Winch then uses in effect eq. (C1) to convert his coefficients into amplitudes and phases of westward- and eastward-moving waves, while Parkinson derives coefficients from the onset for local-time and general terms. The resulting conversion formulas are

$$u_n^m = A_n^m \exp(i\alpha_n^m), \qquad u_n^{-m} = B_n^m \exp(-i\beta_n^m) \tag{C5}$$

with Winch's notation, and

$$u_n^m = \begin{cases} a_n^m - ib_n^m, & p = m \\ c_n^m - id_n^m, & p = m-1 \\ e_n^m - if_n^m, & p = m+1 \end{cases} \tag{C6}$$

with Parkinson's notation, who includes absolute terms with $p = 0$.